

Copepods encounter rates from a model of escape jump behaviour in turbulence

H. Ardeshiri,^{1,2,*} F. G. Schmitt,² S. Souissi,² F. Toschi,^{3,4} and E. Calzavarini¹

¹Univ. Lille, CNRS, FRE 3723, LML, Laboratoire de Mécanique de Lille, F 59000 Lille, France

²Univ. Lille, CNRS, Univ. Littoral Cote d'Opale, UMR 8187, LOG,
Laboratoire d'Océanologie et de Géoscience, F 62930 Wimereux, France

³Department of Applied Physics and Department of Mathematics and Computer Science,
Eindhoven University of Technology, 5600 MB, Eindhoven, The Netherlands

⁴Istituto per le Applicazioni del Calcolo CNR, Via dei Taurini 19, 00185 Rome, Italy

A key ecological parameter for planktonic copepods studies is their interspecies encounter rate which is driven by their behaviour and is strongly influenced by turbulence of the surrounding environment. A distinctive feature of copepods motility is their ability to perform quick displacements, often dubbed jumps, by means of powerful swimming strokes. Such a reaction has been associated to an escape behaviour from flow disturbances due to predators or other external dangers. In the present study, the encounter rate of copepods in a developed turbulent flow with intensity comparable to the one found in copepods' habitat is numerically investigated. This is done by means of a Lagrangian copepod (LC) model that mimics the jump escape reaction behaviour from localised high-shear rate fluctuations in the turbulent flows. Our analysis shows that the encounter rate for copepods of typical perception radius of $\sim \eta$, where η is the dissipative scale of turbulence, can be increased by a factor up to $\sim 10^2$ compared to the one experienced by passively transported fluid tracers. Furthermore, we address the effect of introducing in the LC model a minimal waiting time between consecutive jumps. It is shown that any encounter-rate enhancement is lost if such time goes beyond the dissipative time-scale of turbulence, τ_η . Because typically in the ocean $\eta \sim 10^{-3}$ m and $\tau_\eta \sim 1$ s, this provides stringent constraints on the turbulent-driven enhancement of encounter-rate due to a purely mechanical induced escape reaction.

INTRODUCTION

Many biological processes are determined by individual-interaction or contacts between organisms. This is an essential aspect in plankton marine biology too, because the encounter between individual organisms is vital for mating or for predation [1–3]. Finding a suitable habitat (colonization) for marine organisms is also encounter-dependent [4]. Organism size, morphology, motility and abundance can affect the biological encounter rates, *i.e.*, the typical frequency at which individuals meet other organisms of the same or of different species. Beside this, external environmental factors, such as flow currents and hydrodynamic turbulence can have an impact. It is thus of great ecological importance to understand the combined biological and physical factors that can affect the encounter rates in oceanic flows.

The encounter rate of plankton species has been studied extensively in the past [5–10]. Gerritsen and Strickler [5] first introduced a model of plankton contact rate in a steady uniform flow. Despite its influential role, this model relied on a oversimplified description of the fluid flow environment. The living habitats of plankton, which are open marine flows, are rarely laminar and are instead time-space dependent and frequently turbulent. It is now commonly accepted that turbulence must have an influence on the dispersal, feeding and reproduction of plankton [11]. Furthermore, it is believed that both

small and large eddies of turbulence can affect the encounter process [9].

In the past some authors have regarded the small-scale turbulent processes as a homogenizing factor, so that their encounter-rate models assumed the distribution of plankton to be uniformly random in space and time [10, 12–15]. However, in the fluid-dynamics context it is now well known that turbulence can both increases spatial inhomogeneity at small scales (preferential concentration) and produce persistent clusters over time (this happens for instance for transported scalar fields such as temperature and for material particles carried by a flow)[16–18].

A second important aspect of the problem is that the encounter-rate of swimming organisms in a flow is also governed by biologically-driven processes [10, 19, 20]. Plankton species and in particular copepods each have specific swimming strategies which can be induced by external mechanical stimuli. Some study in the past have assumed that physically-driven (turbulent transport) and biologically-driven (swimming) processes could be summed up linearly in the estimation of encounter-rates [10, 19, 20]. This approach has been questioned on the basis of experimental evidences showing that the two contributions are entangled and most probably depend on each other, in other words: turbulence may induce changes in the behavioural swimming responses of microorganisms [21, 22]. The theoretical model for the estimation of the collision-rate of material particles in turbulence in the conditions leading to preferential clustering, developed by Sundaram and Collins

* hamidreza.ardeshiri@polytech-lille.fr

[23], Wang et al. [24], Reade et al. [25] and Collins and Keswani [26] can be used also for encounter of micro-organisms. Despite the many studies performed on collision enhancement by turbulence for colloidal [27–30], and inertial particles [31, 32], only few studies [33, 34] are available in the context of copepods ecology. The study of Squires and Yamazaki [33] on marine particles did take into account swimming, and the same applies for [34]. Finally it is important to remark that, in addition to swimming behavior induced by changes in external flow conditions, other mechanisms can also play a role in encounter rates for copepods, *e.g.* chemoreception and mechanoreception [35, 36], prey movement detection [37, 38] and feeding currents [39]; all these potentially relevant effects are outside the scope of the present study.

The goal of this work is to offer an estimate of the mutual encounter rate of copepods (encounter rate of the same species) which builds on a previously proposed behavioural model of copepods in a flow [40] (the so called Lagrangian Copepod (LC) model). The LC model was developed from an experimental data analysis input, in order to explore copepods' dynamics in developed turbulent flows. To the best of our knowledge, this is the first numerical simulation of swimming copepods behaviour in turbulent flows which under some specific conditions results in preferential clustering.

MATERIALS AND METHODS

In this section we introduce the Lagrangian copepod model which is adopted in the present study to quantify copepods' encounter-rates in a turbulent flow. This model, which has been first presented in *Ardeshiri et al.* [40], has the advantage to keep into account at the same time a modelisation of behavioural and hydrodynamical effects. The LC model is based on a Eulerian-Lagrangian modelling approach. This means that the fluid flow is obtained by solving the incompressible Navier-Stokes equations, by means of Direct Numerical Simulation (DNS), while the organisms position are treated in the same fashion as Lagrangian point-particles drifting by the flow.

Lagrangian copepod model

The Lagrangian model of copepods dynamics relies both on biological and hydrodynamical assumptions.

i) A first hypothesis is that copepods escape reactions are triggered by a well defined mechanical signal, the strain rate intensity $\dot{\gamma}$, and that a jump begins whenever this signal exceeds a fixed threshold value, denoted with $\dot{\gamma}_T$. The rate of strain intensity is a quantity which depends on the velocity gradients, it is defined as

$\dot{\gamma} = \sqrt{\sum_{i=1}^3 \sum_{j=1}^3 1/2 (\partial_i u_j + \partial_j u_i)^2}$ where u_i is the fluid velocity field in three dimensions ($i = 1, 2, 3$). We note that the strain rate include both normal strain, $\partial_i u_i$, and shear strain, $\partial_j u_i$ ($i \neq j$). In turbulent flows, due to local isotropy, the latter term is the dominant one [41] for this reason we will also refer to $\dot{\gamma}$ as to the shear rate. We also note that the proposed first hypothesis makes several simplifications. In particular it neglects any other copepod swimming activity induced by light, food, or chemistry (*e.g.*, pheromones). Moreover, it neglects the fact that copepod may want to avoid too calm regions of the flow, in other words regions where $\dot{\gamma}$ could be below a certain threshold (a behaviour that has also been reported in the literature [42]).

ii) A second hypothesis is that copepods response is always the same, independently of the intensity of the external mechanical disturbance. There are experimental evidences for the fact that the velocity tracks of copepods performing jumps show always a very sharp velocity increase, followed by an approximately exponential decay in amplitude. This has been highlighted in high-speed recordings for *Eurytemora affinis* and *Acartia tonsa* in still water experiments [40, 43]. Such a functional dependence for the velocity can be associated to the effect of an impulsive force due to a stroke (or a burst of strokes) that is followed by a slowing down due to the hydrodynamic drag force. Furthermore, experiments show that copepods preferentially jumps in their onward direction [44, 45]. This leads to assume that a general template for the time evolution of velocity during a jump can be adopted.

On the mechanical side, the following additional conjectures are made: iii) We assume that copepods are small enough that their center of mass can be considered a perfect fluid tracer in a flow, except for the time when a jump event takes place. In hydrodynamic terms, this means that copepods are assumed to be rigid, homogeneous, neutrally buoyant and with a size that is of the order of the smallest scale of the flow. Neutral buoyancy and mass homogeneity imply that gravity has no role in producing additional acceleration or torque.

iv) Finally, copepods are coupled to the fluid in a one-way fashion, which means that they react and are carried by the flow, but they do not modify it; copepods-copepods interactions are also neglected.

Gathering all the above hypothesis, the LC equation of motion describing a copepod trajectory, $\mathbf{x}(t)$, and its body orientation, $\mathbf{p}(t)$, reads:

$$\dot{\mathbf{x}}(t) = \mathbf{u}(\mathbf{x}(t), t) + \mathbf{J}(t) \quad (1)$$

$$\dot{\mathbf{p}}(t) = \frac{1}{2} \boldsymbol{\omega}(\mathbf{x}(t), t) \wedge \mathbf{p}(t) \quad (2)$$

where $\mathbf{u}(\mathbf{x}(t), t)$ and $\boldsymbol{\omega}(\mathbf{x}(t), t)$ are respectively the velocity and the vorticity of the carrying fluid flow at the copepod position and $\mathbf{J}(t)$ is an added velocity term that describes the jump escape reaction of the copepod, and where \wedge is the vectorial product. We note that eq. (2) is

an accurate description for the rotation rate only for the case of a spherical body, and it is here adopted for simplicity. The generalised form of this equation, valid for axisymmetric ellipsoidal bodies, known as Jeffery equation [46] can also be used (see its effect on the LC model in [40]). The jump term, $\mathbf{J}(t)$, is a function of time but also depends on a set of parameters, which we will introduce and describe in the following. In our model copepods normally drift with the carrier fluid however, when they find themselves in the alert regions, *i.e.* regions with strain rate larger than the reference threshold value $\dot{\gamma}_T$, they perform a jump with exponentially decaying velocity intensity over the time. Notice that a jump has a duration $\tau_w = t_e - t_i$, with t_i and t_e the initial and final time for the jump respectively. Such a time interval can be chosen as the time after which the jump velocity amplitude has declined to a very low value. Note that in our model a new jump cannot occur if the previous jump is not yet finished, this means that the maximal jump rate is τ_w^{-1} (see Fig.1). The jumping event can thus be written as the following expression. When copepods are in alert regions ($\dot{\gamma}(\mathbf{x}(t_i), t_i) > \dot{\gamma}_T$):

$$\mathbf{J}(t, t_i, t_e, \mathbf{p}) = \begin{cases} u_J e^{\frac{t_i - t}{\tau_J}} \mathbf{p}(t_i), & \text{if } t \leq t_e \\ 0, & t > t_e \end{cases} \quad (3)$$

where u_J and τ_J are two parameters characterising the jump shape in terms of, respectively, its velocity amplitude and duration (exponential decay time). Note also that, in the above expression, the jump orientation is identified by $\mathbf{p}(t_i)$ which is the copepod orientation at the time of the jump activation, t_i .

According to the experimental measurements on *Eurytemora affinis* and *Acartia tonsa* [43] a realistic choice for the parameters in the model is $u_J \simeq 10 \text{ cm/s}$ and $\tau_J \simeq 10 \text{ ms}$, respectively. On the contrary our experiments did not allow to estimate the intensity of $\dot{\gamma}_T$ and if any minimal time-interval τ_w between the jumps exists. In the literature we find that $\dot{\gamma}_T$ for *Acartia tonsa* can be around 0.4 s^{-1} [47], however there is a wide range of variability for other species and values as low as $\dot{\gamma}_T = 0.025 \text{ s}^{-1}$ has been also reported [48, 49]. We add here that, if one assumes valid the exponential model for the jump (3), the time needed to reduce the jump amplitude by a factor x is $\tau_w = \ln(x) \tau_J$. Taking then $x = 100$ gives approximately $\tau_w \simeq 50 \text{ ms}$. The uncertainties discussed above on the values of the parameters in the model justify the approach, adopted in this work, of performing a parametric study at varying, independently, $\dot{\gamma}_T$ and τ_w .

Fluid flow model

The natural environment of copepods is characterised by turbulent flows either in the ocean or in river estuaries. Geophysical turbulent flows are often marked by inhomogeneities or by the presence of persistent struc-

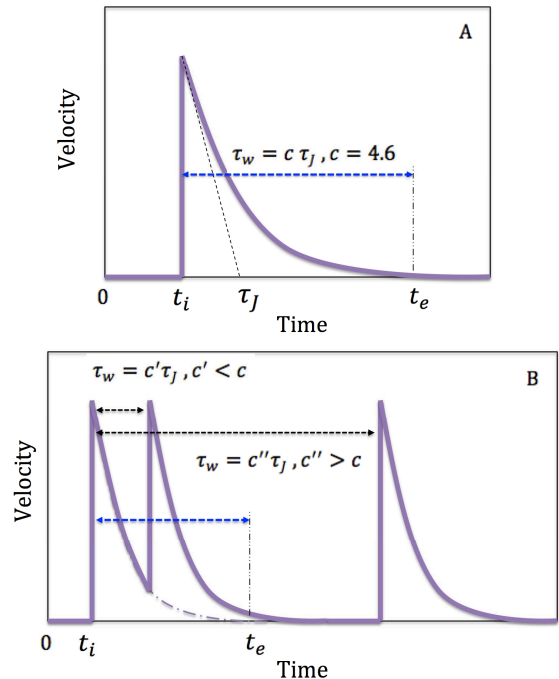


FIG. 1. (A) Cartoon of the functional behaviour of the velocity during a single jump assuming the absence of the fluid velocity. (B) Same as before for two successive jumps at varying the duration of the time interval τ_w between them. Our reference value is here $\tau_w = t_e - t_i = c \tau_J$ with $c = -\ln(10^{-2})$. In the parametric study of section “Effect of waiting time between successive jumps” we vary τ_w in the range $[2, 1000] \tau_J$.

tures due to specific bounding geometries or by the presence of currents. Such aspects are relevant at large scale $O(10 - 10^3)m$, however they lose much of their importance when one looks at fluid fluctuations on a smaller scale, of the order of $1m$. At this level the oceanic turbulence can be taken to a good approximation as statistically homogeneous and isotropic. In such a condition only one parameter suffices to characterise the intensity of turbulence, namely the Taylor-Reynolds number (Re_λ). Re_λ in the ocean can vary from place to place, its most frequent order of magnitude is $Re_\lambda = O(100)$. Typical reference values for the properties of such a turbulent flow are given in table I. In accordance with this picture

Variable	Unit	Value
Kinematic viscosity (ν)	$m^2 s^{-1}$	10^{-6}
Mean velocity fluctuation (u')	ms^{-1}	5×10^{-3}
Turbulent energy dissipation rate (ϵ)	$m^2 s^{-3}$	10^{-6}
Kolmogorov length scale (η)	m	10^{-3}
Kolmogorov time scale (τ_η)	s	1
Kolmogorov velocity scale (u_η)	ms^{-1}	10^{-3}

TABLE I. Order of magnitude estimate for the properties of ocean flow at the Taylor Reynolds number $Re_\lambda \simeq 100$.

and given the fact that the LC model aims at describing copepods' dynamics over a short scale $O(1)m$, we adopt as governing equations of the flow the Navier-Stokes equation for an incompressible flow in three-dimensions, which we solve by means of a Direct Numerical Simulation based on a pseudo-spectral method. The fluid domain is a cubic periodic box. The forcing to sustain the flow acts only at large scale leading to a statistically homogeneous and isotropic turbulence at $Re_\lambda \simeq 80$. The forthcoming discussion on the model results is more conveniently addressed in dimensionless units. The reference scales adopted here will be the dissipative (or Kolmogorov) units: τ_η for time, η for space and $u_\eta = \eta/\tau_\eta$ for the velocity. They are linked by the relation $u_\eta \eta/\nu = 1$, and they represent the smallest scales of the turbulent flow (see the table for an order of magnitude estimate in the ocean). In this units the copepods' jump intensity in our simulation turns out to be $u_J/u_\eta = O(10^2)$, while the copepods' jump decay time is $\tau_J/\tau_\eta = O(10^{-2})$. When the results are analysed in such units, it is expected that the effect of varying Re_λ (increasing the turbulence intensity) will not change significantly the observed phenomena. This is due to the fact that the LC dynamics, its behavioural reaction, but also its patchiness are linked to the dissipative-scales of the turbulent flow [40].

We remark that the above estimate also illustrates the peculiarity of this swimming strategy of copepods. They can impart a velocity that is even larger than the one of the largest vortices in the flow, larger than u' , and this happens over a time which is much shorter than any time scale of the flow. It is clearly an effective way to escape from unwanted locations in the flow. The jump parameter values we use in the simulations presented in this paper, based on our estimates at Re_λ , give $u_J/u_\eta = 250$, while the copepods' jump decay time is $\tau_J/\tau_\eta = 10^{-2}$. Values that we will keep fixed throughout all the present study.

Encounter rate in case of preferential concentration

We look at the single-copepod encounter rate, which is the number of encounters per unit time experienced by one copepod in a population of N individuals in a volume V (number density $n = N/V$). Under the condition of statistically homogeneous and isotropic movement, the single-copepod encounter rate can be written in the following form [23–26, 50, 51]:

$$E(r) = n \, 2\pi r^2 \, g(r) \, \langle \delta v_{rad}(r) \rangle \quad (4)$$

where r is twice the organism's encounter, or perceptive, radius ($r = 2 \, r_p$). Here $g(r)$ represents the pair distribution function, which describes the variation of the particles' density from a reference particle. This has a unit value in the case of homogeneously distributed organisms, while it is greater than one in the condition of local accumulation. Furthermore, for vanishing values of

r it is linked to the fractal dimension of a set of points in space, *i.e.*, the correlation dimension D_2 [52]. The pair distribution function has the following form:

$$g(r) = \frac{1}{4\pi r^2 n N} \sum_{i=1}^N \sum_{j \neq i}^N \delta(r - |\mathbf{r}_{ij}|) \quad (5)$$

where $|\mathbf{r}_{ij}| = |\mathbf{x}_j - \mathbf{x}_i|$ is the Eulerian distance between two particles in a pair (denoted with indexes i and j). The symbol δ denotes here the Dirac generalized function, with $\delta(0) = 1$ and $\delta(x) = 0$ for $x \neq 0$. Finally, $\langle \delta v_{rad}(r) \rangle$ is the mean radial velocity between two organisms separated by the distance r :

$$\langle \delta v_{rad}(r) \rangle = \frac{\sum_{i=1}^N \sum_{j \neq i}^N \left| \dot{\mathbf{r}}_{ij} \cdot \frac{\mathbf{r}_{ij}}{|\mathbf{r}_{ij}|} \right| \delta(r - |\mathbf{r}_{ij}|)}{\sum_{i=1}^N \sum_{j \neq i}^N \delta(r - |\mathbf{r}_{ij}|)} \quad (6)$$

Note that $\dot{\mathbf{r}}_{ij} = \dot{\mathbf{x}}_j - \dot{\mathbf{x}}_i$ denotes here the organisms velocity difference. A detailed explanation on the appropriate choice of the velocity difference to be used in expression (4) can be found in [24]. We finally mention that the total encounter rate, which is the total number of encounters in the population is given by $n \, E(r)$. Non-homogeneous distribution of particles has been studied comprehensively; heavy particles (particles denser than the fluid) concentrate in low vorticity and high strain rate regions [17, 31, 53–56], light particles are trapped by vortices in the flow [17, 31, 56–58], and particles without inertia (fluid passive tracers) are passively advected by the flow. In these cases the observed phenomenon of preferential concentration is controlled by the particles' Stokes number St (which is the ratio of the aerodynamic response time of a particle over the turbulent characteristic time scale, τ_η), and by the density contrast between the particle over the fluid density.

For swimming microorganisms, such as small algae (*e.g.* *chlamydomonas*) which are small and neutrally buoyant, a preferential concentration effect has been found resulting from the gyrotactic motility [59, 60], a competition between the spatial gradients in the fluid velocity, that contributes to the vorticity, and the stabilizing torque due to the displacement of the center of gravity from the center of geometry.

Compared to phytoplankton, copepods show a different type of complexity due to their reactive behavior. Contrary to the previously observed clustering, the patchiness of copepods is tightly linked to their behavioural strategy in turbulent flows; this is the central result in our previous study of the LC model [40].

In the following section the radial distribution function, $g(r)$, its link to the fractal dimension, the radial velocity, $\langle \delta v_{rad}(r) \rangle$, together with their contribution to the encounter rate between copepods will be addressed and discussed in detail.

RESULTS

We organize the analysis in two sections. The first addresses the dependence of encounter rates on the shear rate threshold $\dot{\gamma}_T$ at keeping constant the maximal inter-jump frequency τ_w^{-1} . The second section instead fixes $\dot{\gamma}_T$ and allows τ_w to vary.

Effect of the shear rate threshold

The pair correlation function for the LC model, one of the two main factors in the encounter rate expression (4), is shown in Figure 2 (A). The presence of local copepods concentration is here evident from the fact that $g(r) \gg 1$ at small values of r . Its trend however is non-monotonic with the shear rate threshold parameter. It reaches a peak value (here of about 30) for $\tau_\eta \dot{\gamma}_T = 0.5$, then it decreases. The same trend is observed for the steepness of the decreasing slope of $g(r)$. This reflects what has been previously observed for the correlation dimension D_2 . Indeed it is known that the following relation applies

$$\lim_{r \rightarrow 0} g(r) \sim r^{D_2-3}$$

where 3 stands for the dimension of the physical space. The inset of Fig. 2 reports the $D_2(\dot{\gamma}_T)$ dependence. We remark the value at minimum $D_2 \sim 2.3$ for $\tau_\eta \dot{\gamma}_T = 0.5$, which suggests that copepods may form almost bidimensional, sheet-like structures [40].

The variation of $g(r)$ at different distances (r) is given as a function of the shear rate value in panel (B) of Fig. 2. It is here important to note that the range of $\dot{\gamma}_T$ values, in which the preferential concentration arises is very narrow. $\dot{\gamma}_T$ outside the range $[1/8, 2]\tau_\eta$ leads to almost negligible clustering. Furthermore we see clearly that the largest is the perception radius, the more effective is the preferential clustering mechanism. We may observe that for $r > 10\eta$, which means perception radius larger than 5η we can take $g(r) \simeq 1$.

The mean radial velocity between two copepods at varying $\dot{\gamma}_T$ is shown in Fig. 3. For comparison the same quantity for fluid tracers is also shown. We note that when computed on fluid tracers the radial structure function is an Eulerian quantity which, under the hypothesis of isotropic turbulence, can be related to the better known second-order longitudinal Eulerian structure function via the relation $\langle \delta v_{rad}(r) \rangle = \sqrt{2\langle \delta v_{||}^2(r) \rangle / \pi}$ [56]. If we adopt the empirical approximation given by Borgas and Yeung [61] for $\langle \delta v_{||}^2(r) \rangle$ at finite Re_λ , we find a pretty good agreement with our numerical results. The Eulerian mean radial velocity grows linearly as r^{ζ_d} with $\zeta_d = 1$ for dissipative scales ($r \lesssim 10\eta$) and at inertial-range scales is proportional to r^{ζ_i} with $\zeta_i = 1/3$. From Fig. 3 we see that the jump-rate of copepods with threshold value of $\tau_\eta \dot{\gamma}_T \geq 3.9$ is so low that they behave almost like tracers.

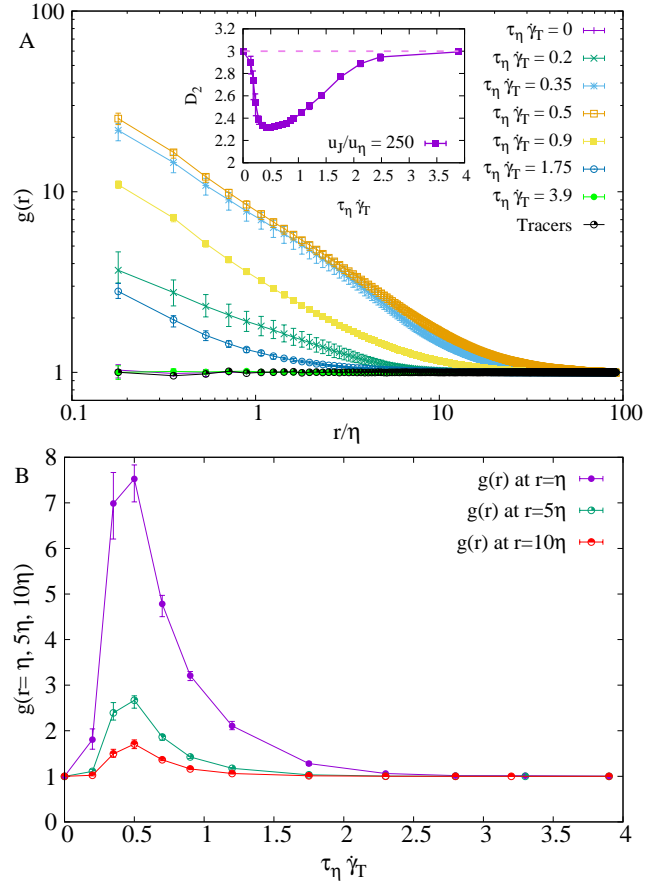


FIG. 2. (A) Pair-radial-distribution function, $g(r)$, for different Lagrangian copepod families with different threshold values of the shear rate $\tau_\eta \dot{\gamma}_T$. The inset represents the correlation dimension of copepod distribution with jump intensity, $u_J/u_\eta = 250$ and $\tau_J/\tau_\eta = 10^{-2}$. (B) Variation of $g(r)$ at different distances as a function of the threshold $\dot{\gamma}_T$.

They are thus passively advected by the flow and, for this reason, they go very close to the prediction just given for tracers. By decreasing the shear rate threshold value, copepods become more and more reactive, therefore the jumping part in the mean radial velocity expression becomes increasingly dominant. In the case where all copepods are permanently in alert regions ($\dot{\gamma}_T = 0$) one can expect a Brownian-like motion of copepods according to the LC model. For this case, copepod's relative velocity tends to be constant over space and its amplitude is proportional to the jump intensity (u_J). If we assume that the jumps for different copepods are uncorrelated both in time and in space and that the additional fluid velocity is negligible one can easily compute the level value of this plateau (see Fig. 3). By dimensional reasoning one can show that in the latter case the effective diffusivity of the copepods is proportional $u_J^2 \tau_J$. For other cases (intermediate shear rate threshold values $\tau_\eta \dot{\gamma}_T$) the behaviour is more complicated and difficult to capture by analytical or dimensional arguments. We observe that in the limit of $r \rightarrow 0$ the mean radial velocity function, $\langle \delta v_{rad}(r) \rangle$,

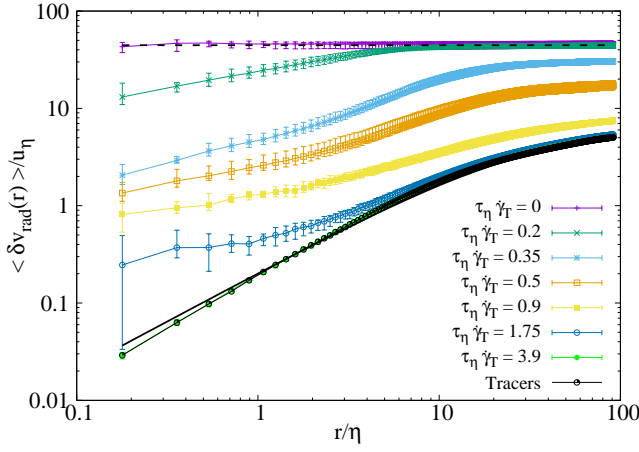


FIG. 3. Dimensionless mean radial velocity, $\langle \delta v_{rad}(r) \rangle / u_\eta$ between couples of Lagrangian copepods separated by a distance r/η for different values of the threshold strain rate intensity $\dot{\gamma}_T$. The continuous line is the prediction for fluid tracers based on the empirical approximation on the second-order longitudinal Eulerian structure function proposed by Borgas and Yeung [61]. The dashed line plateau indicates the prediction derived from a random field of spatially and temporally uncorrelated jumps.

goes to zero for fluid tracers but it has non-zero value for different families of copepods and is more pronounced by decreasing the shear rate threshold value. This pattern is caused by singularities in the copepods dynamics which implies that copepods at distance r may have a different behaviour, hence a different velocity. In the field of particle laden flows this discontinuity in the particle velocity field is often referred to as a caustic singularity [62, 63]. This is better illustrated in the visualisation of Fig. 4 where pairs of very close copepods may have very large velocity differences.

Finally, we remark that differently from the trend observed for $g(r)$ the behaviour of $\langle \delta v_{rad}(r) \rangle$ is inversely proportional and monotonic with $\dot{\gamma}_T$: at increasing the shear rate threshold the mean radial velocity difference goes down from the plateau level to the fluid tracer level. The scaling exponents ζ_d, ζ_i of $\langle \delta v_{rad}(r) \rangle$ for different copepod families at varying $\dot{\gamma}_T$ are obtained via power law fits are shown in Fig. 5. The change of the power law scaling exponent in the inertial-range is smooth, but at the dissipative scale it shows a non monotonic behaviour for the fractal dimension as a function of the shear rate threshold values, as already reported for the pair correlation function in Fig. 2.

Having the pair correlation function, $g(r)$, and the mean radial velocity, $\delta v_{rad}(r)$, one can estimate the encounter rate kernel, $E(r)$. There is of course no contact between tracers, because they are size-less by definition and are passively advected by an incompressible flow, where the fluid streamlines does not cross each other. However, when a virtual radial size R is assigned to a tracer, their virtual contact rate is proportional to the mean radial velocity evaluated at $r = 2R$. Copepods differs from

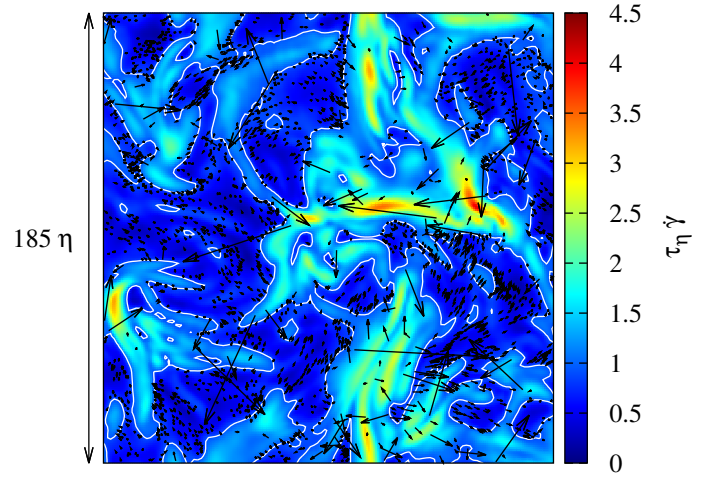


FIG. 4. Visualisation of the instantaneous spatial distribution of Lagrangian copepods in turbulent flow along with their velocity vectors. The data here comes from a two-dimensional slice, of spatial lateral dimensions $185\eta \times 185\eta$ and thickness η , out of the simulated $(185\eta)^3$ three-dimensional domain. The velocity vectors are in a arbitrary scale. The copepods are characterised by the parameter set: $u_J = 250u_\eta$, $\tau_J = 10^{-2}\tau_\eta$, $\dot{\gamma}_T = 0.91 \tau_\eta^{-1}$ and $\tau_w = 4.6\tau_J$. The color map represents the instantaneous Eulerian field of the absolute value of the strain rate, $|\dot{\gamma}|$. Contour lines are traced for the threshold value $\dot{\gamma} = \dot{\gamma}_T$, hence it traces the boundaries between comfort and alert regions in the flow (respectively light and dark shaded regions).

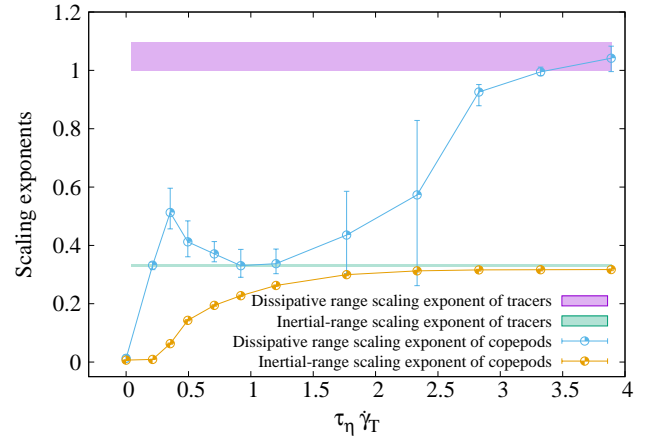


FIG. 5. Scaling exponents of $\langle \delta v_{rad}(r) \rangle$ vs. r from power law fits in the dissipative (r/η in range $[0.15, 2.5]$), r^{ζ_d} , and inertial-range limit (r/η in range $[35, 100]$), r^{ζ_i} . Error bars on exponents have been estimated by shifting the fitting window towards lower and higher value.

tracers in two aspects, first they are not simply passively transported by the flow and secondly their virtual contact rate, called radius of perception, has a specific biological meaning. It is known that copepods-copepods or copepods-prey/food interactions occurs before the possible body-to-body physical contact: copepods can grab

their prey or become aware of an incoming mate before hit them [34]. This is why R should be understood as twice the radius of perception of the organisms rather than their geometrical size.

Fig. 6 reports the encounter kernel as a function of r for different copepod families. Here the encounter rate of tracers are traced as for comparison with the different copepod families. It appears that by increasing the shear rate threshold value ($\tau_\eta \dot{\gamma}_T$) the encounter rate of copepods decreases monotonically, although the growth of the shear rate $\tau_\eta \dot{\gamma}_T$ had non-uniform impact on the pair correlation dimension (see Fig. 2). This implies that the dominant term in interspecies encounter rate of the copepods is the amplitude of their mean radial velocity. The encounter rate is dominated by caustics.

The vertical line in the figure shows the radius of perception for Lagrangian copepod particles, here supposed to be 5 times greater than the Kolmogorov length scale of the carrier fluid. The ratio of the radius of perception to the copepods' body size is reported to be in the range 1 – 3 [64–66]. In terms of η this means that the radius of perception of copepods is of the order of ~ 1 . In order to see how effective the shear rate threshold value is on the encounter rate of Lagrangian copepods at different perception radius, one can estimate the ratio between the encounter rates experienced by copepod families and tracers. This is shown in Fig. 7 where it is realistic to have larger encounter rates at small distances. This figure suggests that at optimum clustering, corresponding to the shear rate threshold value of $\tau_\eta \dot{\gamma}_T = 0.5$, the encounter rate can be of the order of ~ 10 with respect to the tracers at distance $r = 5\eta$. The LC model shows no contact rate enhancement at shear rate values larger than 2.75. This means that when $\dot{\gamma} > 2.75/\tau_\eta$ then there is any increase of contact rate between copepods due to their swimming behaviour. Therefore, dimensionally the LC model do not give any significant advantage at $\dot{\gamma} > 2.75 s^{-1}$. When the shear rate $\dot{\gamma}$ is lowered, the contact rate reaches up to 100 times the value of fluid tracers. Notice however that copepod-copepod interaction has been neglected in the LC model, and this may have lead to large overestimation of contact-rates.

Effect of waiting time between successive jumps

Up to now we assumed that a copepod's jump was terminated after a prescribed time interval τ_w from the jump inception, defined it as when the jump velocity amplitude reaches one percent of the copepods' initial jump intensity. In reality copepods can behave differently. For instance they can be less reactive of what has been modeled so far since they have some finite energy amount available for swimming and after repeated jumps they may need some time in order to recover their lost energy [67]. The probability density function of time between successive jumps (not shown here) indicates the presence of memory on the previous jumps of copepods (see also

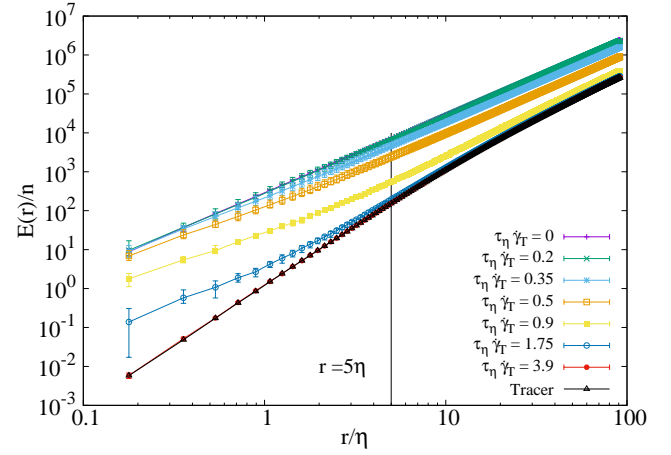


FIG. 6. Encounter rate per unit particle density for different Lagrangian copepod families with different values of deformation-rate threshold $\dot{\gamma}_T$.

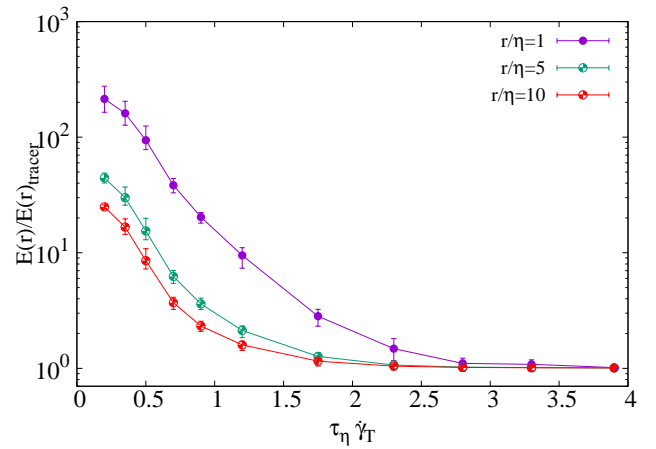


FIG. 7. Ratio between encounter rates experienced by Lagrangian copepod particles and the one experienced by fluid tracer particles with the same perception radius.

[68]) but there is a lack of quantitative elements in order to have enough information to model this feature in the LC model.

We now vary the duration of the waiting time, taking as a reference the family for which $\tau_w/\tau_J = c$ with $c = 4.6$ (a family with $u_J/u_\eta = 250$, $\tau_J/\tau_\eta = 10^{-2}$ and $\dot{\gamma}_T = 0.5$ where a complete jump lasts for 46 ms) as shown in blue in Fig. 8. We now have Lagrangian copepod families with $u_J/u_\eta = 250$, $\tau_J/\tau_\eta = 10^{-2}$, $\dot{\gamma}_T = 0.5$ and τ_w/τ_J which varies in range $[0.5c, 200c]$.

Fig. 8 interestingly shows that by making copepods progressively less reactive, the small scale clustering, characterised by D_2 , fades away and only a prompt copepod reactions may lead to non-homogenous spatial distribution. Moreover, when the waiting time, τ_w , is larger than the Kolmogorov time scale of the flow, τ_η , copepods' spatial distribution becomes nearly homogenous. It is now interesting to see how these changes in spatial distribution can affect the encounter rate. In Fig. 9 the en-

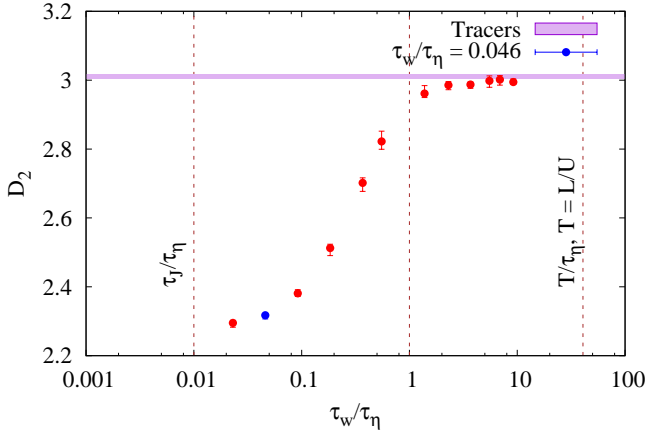


FIG. 8. Effect of the waiting time between successive jumps on the correlation dimension. Blue dot corresponds to the copepods family with $u_J/u_\eta = 250$, $\tau_J/\tau_\eta = 10^{-2}$, $\dot{\gamma}_T = 0.5\tau_\eta^{-1}$ and $\tau_w/\tau_\eta = 0.046$ for which optimal clustering happened. The vertical dashed lines show the τ_J/τ_η , τ_w/τ_η and the ratio between the large eddy turnover time of the flow, T , and Kolmogorov time scale, τ_η , from left to right. Note that in this test $\dot{\gamma}_T = 0.5\tau_\eta^{-1}$ is kept fixed and corresponds to the case with maximum small scale clustering.

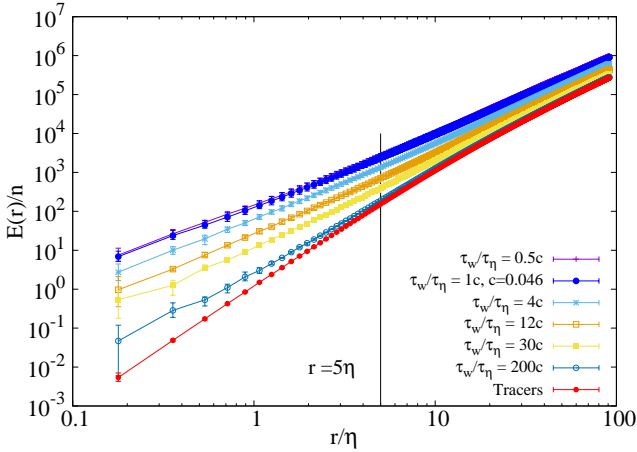


FIG. 9. Encounter rate per unit particle density for different Lagrangian copepod families with different waiting time between successive jumps, τ_w/τ_η (all other parameters are the same as in previous figure).

counter rate per unit particle density as a function of r is shown for different Lagrangian copepod families that we observed in Fig. 8. One can normalize the encounter rate experienced by copepod families by the one of tracers at a specific perception radius in order to clearly see the effect of waiting time between successive jumps. This is shown in Fig. 10 where it is seen that the increase of the waiting time decreases the copepods' encounter rates. For $\tau_w \simeq 2\tau_\eta$ the encounter rate enhancement as compared to tracers is just a factor ~ 8 for $r = \eta$ and decrease to nearly a factor ~ 2 for $r = 5\eta$.

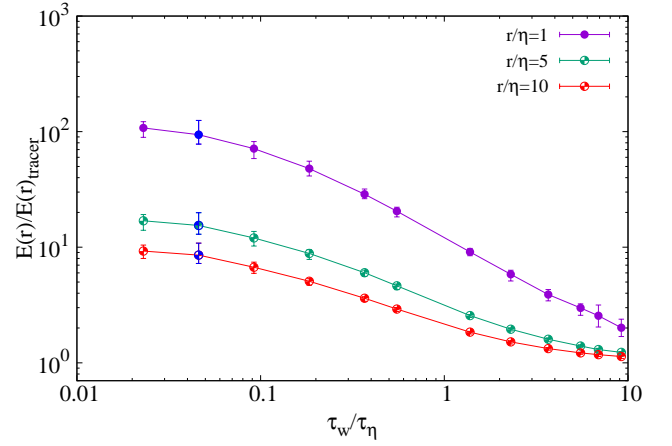


FIG. 10. Ratio between encounter rates experienced by Lagrangian copepod particles and the one experienced by fluid tracer particles with the same perception radius as a function of waiting time between successive jumps. The filled symbols correspond to the copepods family with $\tau_w/\tau_J = c$ at different perception radius.

DISCUSSION

The model for copepods dynamics in turbulence studied in this paper leads to an enhancement of the encounter rate. This increase has its origin in two distinct mechanisms: the preferential concentration, quantified by $g(r)$, and the mean approaching velocity difference, measured by $\delta v_{rad}(r)$. The parametric analysis at varying $\dot{\gamma}_T$ reveals that the lower is the threshold the higher is the encounter rate. A similar result is found for the investigation at fixed $\dot{\gamma}_T = 0.5\tau_\eta^{-1}$ and at varying inter-jump minimal time τ_w : the shorter is the time, the more frequent are the encounters. These results are easy to grasp. A very reactive organism will explore much more space than a nearly passive one and will enhance its chances to meet similar organisms. However, one may want to ask if, despite its simplicity, the LC model can provide also a non trivial insight on the possible dynamics of copepods in turbulence.

A first significant observation is that the dissipative scale, τ_η , is the relevant control scale for the encounter rate enhancement. It defines respectively both the reference frequency and the reference time gap for $\dot{\gamma}_T$ and τ_w . In other words the present mechanisms of enhancement of encounters is effective only if copepods have a shear rate sensitivity that is finer than the shear rate produced at the Kolmogorov scale $\sim \tau_\eta^{-1}$ and if their jumps occurs at a rate higher than this very same frequency. In dimensional terms this corresponds to $\tau_\eta^{-1} \simeq 1s^{-1}$, however, due to the difference turbulent conditions found in the ocean, it is known it might have more than one decade range of variability (from 0.1 to 10 s^{-1} as from [69]). The fact that the shear rate threshold value to trigger a jump in copepods has been reported to vary from $\dot{\gamma}_T = 0.025 s^{-1}$ [48, 49] to $\dot{\gamma}_T = 0.4 s^{-1}$ [47], seems to

support the validity of the model findings. A second observation is that the enhancement of contact rate by the present mechanism is much less effective when the perception radius is wider. We note the large gap existing between the estimated encounter rates at $r = \eta$ and $r = 10\eta$. This has a biological relevance: Larger copepods or copepods simply with a longer range perception are less affected by the preferential concentration mechanisms and by the increase of the approaching velocity. This also set a quantitative limit, if $r \geq 10\eta \simeq 1\text{cm}$ the effect of encounter rate enhancement by turbulence is negligible. The fact that the radius of perception to copepods is in the *mm* range [64–66] suggests that the proposed mechanisms may be effective at least for small copepod species. A complementary interpretation of this result is that for a copepod family of a given perception radius, the turbulence induced enhancement of encounter rates is less and less effective as the the turbulent intensity is increased, and is much effective at moderate levels of turbulence.

We now discuss possible limitations of the model and potential features that we neglected and that may change the scenario described so far. One shortcoming of the model is the fact that we do not take into account the energetics of copepods. It is unlikely that these organisms may jump indefinitely at a maximum rate τ_w^{-1} , even if such a rate is not sustained. It is more likely that periods of high activity will be followed by a resting time. A realistic energetic model for copepods could lead to slightly different quantitative estimates for $E(r)$ however it will not modify the observation that τ_η is a characteristic scale of the problem. Another limitation concerns the absence of a post-encounter dynamics in our model. The Lagrangian copepods we simulate can have trajectories that cross each others and do not bounce or react differently when they encounter each other (we talk in this case of virtual encounters). In reality we expect different behaviour in the moments following an encounter. This may lead to substantial different conclusions and we think it will be interesting to include this feature as a refinement of the present model.

Conclusion

This paper address the problem of the quantification of inter-species contact rate in copepods in field conditions. The copepods habitat is sea water flow characterised by large scale currents and turbulence with variable intensities. The copepods' encounter rate is certainly influenced by this turbulence environment, but on the

other hand copepods are also known to be capable to displace quickly when locally subjected to mechanical disturbances. The way in which environment and this single, specific, behavioural conditions combines is complex. In this paper we couple the exact dynamics of homogeneous and isotropic turbulent flows, by using DNS, with a simplistic model of behaviour where copepods jumps are triggered by localized high strain events. The main result of this investigations lies in the enhanced interspecies contact rate with respect to the case where copepods are considered as fluid tracer particles. This enhancement comes from two terms in the contact rate expression; one is the variation of the pair correlation function $g(r)$ which accounts for the spatial preferential concentration and the other one is the variation of the mean approaching velocity $\langle \delta v_{rad}(r) \rangle$, which comes from the fact that copepods can have an independent swim velocity. Our analysis shows that the encounter rate for copepods of typical perception radius of $O(\eta)$, where η is the dissipative scale of turbulence, can be increased by a factor up to $\sim 10^2$ compared to the one experienced by passively transported fluid tracers, a very large value, which can be ecologically important. Such effect may show that jumping behaviour of copepods is ecologically justified not only to avoid predators, but also to increase the mating encounter rate. Furthermore, the study of a minimal pause interval between consecutive jumps shows that any encounter-rate enhancement is lost if such time goes beyond the dissipative time-scale of turbulence τ_η . This provides relevant constraints on the turbulent-driven enhancement of contact-rate due to a purely mechanic induced escape reaction.

We conclude by remarking that the large enhancement of the contact rate highlighted in this paper, while relevant for mating behaviour of copepods it is less relevant for prey capture estimates. As a perspective it would be interesting to see the consequence of our LC model for the feeding behaviour by using the Lagrangian model of copepods one side and larger bodies drifting in the flow which can model the presence of large predators.

FUNDING

This study is part of the PhD thesis of H. Ardeschiri. This work was financially supported by a grant for interdisciplinary research “Allocation President 2013” of the Université de Lille 1. The authors would like to acknowledge networking support by COST Action MP1305 “Flowing matter”. E.C. thanks Haitao Xu for useful discussions.

[1] A. M. Hein and S. A. McKinley, “Sensory information and encounter rates of interacting species,” *PLOS Com-*

- [2] S. Menden-Deuer, "An integrated model simulation and empirical laboratory on biological encounter rates," *Oceanography* **19**, 185–189 (2006).
- [3] T. Kiørboe, *A Mechanistic Approach to Plankton Ecology* (Princeton University Press, 2008).
- [4] M. E. Wosniack, M. C. Santos, M. R. Pie, M. C. M. Marques, E. P. Raposo, G. M. Viswanathan, and M. G. E. da Luz, "Unveiling a mechanism for species decline in fragmented habitats: fragmentation induced reduction in encounter rates," *Journal of The Royal Society Interface* **11**, 20130887 (2014).
- [5] J. Gerritsen and J. R. Strikler, "Encounter probabilities and community structure in zooplankton: a mathematical model," *Journal of the Fisheries Research Board of Canada* **34**, 73–82 (1977).
- [6] B. J. Rothschild and T. R. Osborn, "Small-scale turbulence and plankton contact rates," *Journal of Plankton Research* **10**, 465–474 (1988).
- [7] G. T. Evans, "The encounter speed of moving predator and prey," *Journal of Plankton Research* **11**, 415–417 (1989).
- [8] B. R. MacKenzie, T. J. Miller, S. Cyr, and W. C. Leggett, "Evidence for a dome shaped relationship between turbulence and larval fish ingestion rates," *Limnology and Oceanography* **39**, 1790–1799 (1994).
- [9] A. W. Visser and B. R. MacKenzie, "Turbulence-induced contact rates of plankton: the question of scale," *Journal of Plankton Research* **166**, 307–310 (1998).
- [10] T. Kiørboe and E. Saiz, "Planktivorous feeding in calm and turbulent environments, with emphasis on copepods," *Marine Ecology Progress Series* **122**, 135–145 (1995).
- [11] H. L. Pécseli, J. Trulsen, and Ø. Fiksen, "Predator-prey encounter and capture rates for plankton in turbulent environments," *Progress in Oceanography* **101**, 14–32 (2012).
- [12] S. Sundby and P. Fossum, "Feeding conditions of arctonorwegian cod larvae compared with the rothschild-osborn theory on small-scale turbulence and plankton contact rates," *Journal of Plankton Research* **12**, 1153–1162 (1990).
- [13] C. S. Davis, G. R. FLierl, P. H. Wiebe, and P. J. S. Franks, "Micropatchiness, turbulence and recruitment in plankton," *Journal of Marine Research* **49**, 109–151 (1991).
- [14] B. R. MacKenzie and W. C. Leggett, "Quantifying the contribution of small-scale turbulence to the encounter rates between larval fish and their zooplankton prey: effects of wind and tide," *Marine Ecology Progress Series* **73**, 149–160 (1991).
- [15] P. Caparroy and F. Carlotti, "A model for acartia tonsa: effect of turbulence and consequences for the related physiological processes," *Journal of Plankton Research* **18**, 2139–2177 (1996).
- [16] U. Frisch, *Turbulence: The Legacy of A. N. Kolmogorov*. (Cambridge University Press, 1995).
- [17] F. Toschi and E. Bodenschatz, "Lagrangian properties of particles in turbulence," *Annual Review of Fluid Mechanics* **41**, 375–404 (2009).
- [18] F. G. Schmitt and Y. Huang, *Stochastic Analysis of Scaling Time Series: From Turbulence Theory to Applications* (Cambridge University Press, 2016).
- [19] L. Seuront, F. G. Schmitt, and Y. Lagadeuc, "Turbulence intermittency, small-scale phytoplankton patchiness and encounter rates in plankton: where do we go from here?" *Deep-Sea Research Part I* **48**, 1199–1215 (2001).
- [20] L. Dzierzbicka-Glowacka, "Encounter rates in zooplankton," *Polish Journal of Environmental Studies* **15**, 243–257 (2006).
- [21] C. P. Jennifer, R. S. Kelly, J. N. Kerry, and M. K. Amanda, "Biophysical interactions in the plankton: A cross-scale review," *Limnology and Oceanography* **2**, 121–145 (2012).
- [22] W. M. Durham and R. Stocker, "Thin phytoplankton layers: Characteristics, mechanisms, and consequences," *Annual Review of Marine Science* **4**, 177–207 (2012).
- [23] S. Sundaram and L. R. Collins, "Collision statistics in an isotropic particle-laden turbulent suspension. part 1. direct numerical simulations," *Journal of Fluid Mechanics* **335**, 75–109 (1977).
- [24] L. P. Wang, A. S. Wexler, and Y. Zhou, "Statistical mechanical descriptions of turbulent coagulation," *Physics of Fluids* **10**, 2647–2651 (1998).
- [25] W. C. Reade and L. R. Collins, "Effect of preferential concentration on turbulent collision rates," *Physics of Fluids* **12**, 2530–2540 (2000).
- [26] L. R. Collins and A. Keswani, "Reynolds number scaling of particle clustering in turbulent aerosols," *New Journal of Physics* **6**, 119 (2004).
- [27] L. P. Wang, A. S. Wexler, and Y. Zhou, "Statistical mechanical description and modelling of turbulent collision of inertial particles," *Journal of Fluid Mechanics* **415**, 117–153 (2000).
- [28] H. Lian, G. Charalampous, and Y. Hardalupas, "Preferential concentration of poly-dispersed droplets in stationary isotropic turbulence," *Experiments in Fluids* **54**, 1525 (2013).
- [29] G. Falkovich, A. Fouxon, and M. G. Stepanov, "Acceleration of rain initiation by cloud turbulence," *Nature* **419**, 151–154 (2002).
- [30] B. K. Brunk, D. L. Koch, and L. W. Lion, "Turbulent coagulation of colloidal particles," *Journal of Fluid Mechanics* **364**, 81–113 (1998).
- [31] K. D. Squires and J. K. Eaton, "Preferential concentration of particles by turbulence," *Physics of Fluids* **3**, 1169–1178 (1991).
- [32] R. Monchaux, M. Bourgoïn, and A. Cartellier., "Preferential concentration of heavy particles: A voronoi analysis," *Physics of Fluids* **22**, 103304 (2010).
- [33] K. D. Squires and H. Yamazaki, "Preferential concentration of marine particles in isotropic turbulence," *Deep Sea Research Part I: Oceanographic Research Papers* **42**, 1989–2004 (1995).
- [34] F. G. Schmitt and L. Seuront, "Intermittent turbulence and copepod dynamics: Increase in encounter rates through preferential concentration," *Journal of Marine Systems* **70**, 263–272 (2008).
- [35] E. J. Buskey, "Swimming pattern as an indicator of the roles of copepod sensory systems in the recognition of food," *Marine Biology* **79**, 165–175 (1984).
- [36] M. J. Weissburg, M. H. Doall, and J. Yen, "Following the invisible trail: kinematic analysis of mate-tracking in the copepod temora longicornis," *Philosophical transactions of the Royal Society of London* **353**, 701–712 (1998).
- [37] A. W. Visser, "Hydromechanical signals in the plankton," *Marine Ecology Progress Series* **222**, 1–24 (2001).

- [38] H. Jiang, T. R. Osborn, and C. Meneveau, "Hydrodynamic interaction between two copepods: a numerical study," *Journal of Plankton Research* **24**, 235–253 (2002).
- [39] C. Marrasé, J. H. Costello, T. Granata, and J. R. Strickler, "Grazing in a turbulent environment: energy dissipation, encounter rates, and efficacy of feeding currents in centropages hamatus," *PNAS, Proceedings of the National Academy of Sciences* **87**, 1653–1657 (1990).
- [40] H. Ardeshiri, I. Benkaddad, F. G. Schmitt, S. Souissi, F. Toschi, and E. Calzavarini, "Lagrangian model of copepod dynamics: Clustering by escape jumps in turbulence," *Physical Review E* **93**, 043117 (2016).
- [41] J. O. Hinze, *Turbulence* (McGraw-Hill, 1975).
- [42] E. Saiz and T. Kiørboe, "Predatory and suspension feeding of the copepod acartia tonsa in turbulent environments," *Marine Ecology Progress Series* **122**, 147–158 (1995).
- [43] H. Ardeshiri, "Dynamics of copepods in turbulent flows," PhD dissertation, Lille 1 University of Science and Technology (2016).
- [44] E. J. Buskey, P. H. Lenz, and D. K. Hartline, "Escape behavior of planktonic copepods in response to hydrodynamic disturbances: high speed video analysis," *Marine Ecology Progress Series* **235**, 135–146 (2002).
- [45] E. J. Buskey and D. K. Hartline, "High-speed video analysis of the escape responses of the copepod acartia tonsa to shadows," *The Biological Bulletin* **204**, 28–37 (2003).
- [46] G. Jeffery, "The motion of ellipsoidal particles immersed in a viscous fluid," *Proceedings of the Royal Society of London. Series A, Containing Papers of a Mathematical and Physical Character* **102**, 161–179 (1992).
- [47] T. Kiørboe, E. Saiz, and A. Visser, "Hydrodynamic signal perception in the copepod acartia tonsa," *Marine Ecology Progress Series* **179**, 97–111 (1999).
- [48] C. B. Woodson, D. R. Webster, M. J. Weissburg, and J. Yen, "Response of copepods to physical gradients associated with structure in the ocean," *Limnology and Oceanography* **50**(5), 1552–1564 (2005).
- [49] C. B. Woodson, D. R. Webster, M. J. Weissburg, and J. Yen, "Cue hierarchy and foraging in calanoid copepods: ecological implications of oceanographic structure," *Marine Ecology Progress Series* **330**, 163–177 (2007).
- [50] P. G. Saffman and J. S. Turner, "On the collision of drops in turbulent clouds," *Journal of Fluid Mechanics* **1**, 16–30 (1956).
- [51] R. Onishi and J. C. Vassilicos, "Collision statistics of inertial particles in two-dimensional homogeneous isotropic turbulence with an inverse cascade," *Journal of Fluid Mechanics* **745**, 279–299 (2014).
- [52] P. Grassberger and I. Procaccia, "Measuring the strangeness of strange attractors," *Physica D: Nonlinear Phenomena* **9**, 189–208 (1983).
- [53] M. R. Maxey, "The gravitational settling of aerosol particles in homogeneous turbulence and random flow fields," *Journal of Fluid Mechanics* **174**, 441–465 (1987).
- [54] L. P. Wang and M. R. Maxey, "Settling velocity and concentration distribution of heavy particles in homogeneous isotropic turbulence," *Journal of Fluid Mechanics* **256**, 27–68. (1993).
- [55] J. R. Fessler, J. D. Kullick, and J. K. Eaton, "Preferential concentration of heavy particles in a turbulent channel flow," *Physics of Fluids* **6**, 3742–3749 (1994).
- [56] L.I. Zaichik, V.M. Alipchenkov, and A.R. Avetissian, "Modelling turbulent collision rates of inertial particles," *International Journal of Heat and Fluid Flow* **27**, 937–944 (2006).
- [57] E. Calzavarini, M. Kerscher, D. Lohse, and F. Toschi, "Minkowski functionals: characterizing particle and bubble clusters in turbulent flow," *Journal of Fluid Mechanics* **607**, 13–24 (2008).
- [58] E. Calzavarini, T. H. van den Berg, F. Toschi, and D. Lohse, "Quantifying microbubble clustering in turbulent flow from single-point measurements," *Physics of Fluids* **20**, 040702 (2008).
- [59] W. M. Durham, E. Climent, M. Barry, F. De Lillo, G. Boffetta, M. Cencini, and R. Stocker, "Turbulence drives microscale patches of motile phytoplankton," *Nature Communication* **4**, 1–7 (2013).
- [60] F. De Lillo, M. Cencini, W. M. Durham, M. Barry, R. Stocker, E. Climent, and G. Boffetta, "Turbulent fluid acceleration generates clusters of gyrotactic microorganisms," *Physical Review Letters* **112**, 044502 (2014).
- [61] M. S. Borgas and P. K. Yeung, "Relative dispersion in isotropic turbulence. part 2. a new stochastic model with reynolds-number dependence," *Journal of Fluid Mechanics* **503**, 125–160 (2004).
- [62] A. Crisanti, M. Falcioni, A. Provenzale, P. Tanga, and A. Vulpiani, "Dynamics of passively advected impurities in simple two-dimensional flow models," *Physics of Fluids* **4**, 1805–1820 (1992).
- [63] K. Gustavsson, E. Meneguz, M. Reeks, and B. Mehlig, "Inertial-particle dynamics in turbulent flows: caustics, concentration fluctuations and random uncorrelated motion," *New Journal of Physics* **14**, 115017 (2012).
- [64] P. H. Lenz and J. Yen, "Distal setal mechanoreceptors of the first antennae of marine copepods," *Bulletin of Marine Science* **53**, 170–179 (1993).
- [65] E. Bagoien and T. Kiørboe, "Blind dating-mate finding in planktonic copepods. i. tracking the pheromone trail of centropages typicus," *Marine Ecology Progress Series* **300**, 105–115 (2005).
- [66] M. H. Doall, S. P. Colin, J. R. Strickler, and J. Yen, "Locating a mate in 3d: the case of temora longicornis," *Philosophical transactions of the Royal Society of London, Series B* **353**, 681–689 (1998).
- [67] A. W. Visser and U. H. Thygesen, "Random motility of plankton: diffusive and aggregative contributions," *Journal of Plankton Research* **25**, 1157–1168 (2003).
- [68] G. Dur, S. Souissi, F. Schmitt, S. Cheng, and J. S. Hwang, "The different aspects in motion of the three reproductive stages of pseudodiaptomus annandalei (copepoda, calanoida)," *Journal of Plankton Research* **32**, 423–440 (2010).
- [69] J. Jiménez, "Oceanic turbulence at millimeter scales," *SCI. MAR.* **61**, 47–56 (1997).